Check for updates

Divergent response of *Pinus pumila* growth to climate warming at different latitudes and in different simulation predictions

Jingwen Yang[1,2,3], Qiuliang Zhang[2], Wenqi Song[3], Yang An[4] and Xiaochun Wang[1,3]*

[1]School of Life, Qufu Normal University, Qufu, China, [2]College of Forestry, Inner Mongolia Agricultural University, Hohhot, China, [3]Center for Ecological Research and Key Laboratory of Sustainable Forest Ecosystem Management-Ministry of Education, College of Forestry, Northeast Forestry University, Harbin, China, [4]Chang'an Park in Shijiazhuang, Shijiazhuang, China

Understanding the responses of shrub growth to climate changes is key to accurately predicting the dynamic changes in the boreal forest ecosystem. A shrub-ring network based on 12 sites was established to explore the response of *Pinus pumila* growth to climate change in northeastern China. The sampling sites are distributed along the latitudinal gradient of 44.10° to 52.58° and were divided into three regions: south, central, and north. The results show that there have been significant differences in *P. pumila* growth trends at different latitudes in recent decades. From 1950 to 1980, *P. pumila* in the southern and central regions grew faster than in the northern region. From 1981 to 2014, however, the growth of *P. pumila* increased in the north but slowed in the south and central regions. The temperatures of the previous winter and current spring are the main factors limiting the growth of *P. pumila* in the north and south. In the central and southern regions, the growth of *P. pumila* is negatively correlated with precipitation of the previous and current summers. In the north, summer temperatures from 1981 to 2014 gradually inhibit the growth of *P. pumila*, while summer precipitation has a positive impact on growth. Our model indicates that the radial growth trend of *P. pumila* in the north is likely to decline as the climate warms. Surprisingly, the growth of *P. pumila* in the south is predicted to benefit from warming under the RCP4.5, RCP6.0, and RCP8.5 scenarios. Therefore, *P. pumila* may not expand northward in the context of climate warming.

KEYWORDS

climate change, boreal, shrub, latitude, *Pinus pumila*

1 Introduction

Projected global warming of 2.4°C to 3.5°C by 2100 is expected to lead to alpine glacier retreat, snow cover reduction, and large-scale precipitation changes, significantly impacting ecosystem dynamics and social communities (IPCC, 2021). There is increasing evidence that recent climate change has affected the ecological performance of global plant species, from phenology, growth, and reproductive investment to recruitment rates (Jump et al., 2006; Matías et al., 2017; Fang and Zhang, 2019). Global warming influences the growth, distribution, and regeneration dynamics of shrubs (Kueppers et al., 2017). Dwarf shrub species usually grow above the treeline or timberline and may experience the highest warming rate in places where tall tree species are rarely distributed (Shetti, 2018; Lu et al., 2021). They play an irreplaceable role in forest water conservation, sand fixation, soil improvement, and ecological balance (Xiao et al., 2019).

The impact of climate warming on shrub growth response is not limited to distribution changes; it also influences radial and axial growth. Previous studies have shown that shrub rings provide insights into the impact of climate change on boreal forest and dryland ecosystems (Fang et al., 2001; Gauthier et al., 2015; Shetti, 2018; Buchwal et al., 2020). Shrub ring widths can be used to indicate long-term moisture and temperature at high altitudes and latitudes (Myers-Smith et al., 2020). In recent years, research on the use of "shrubchronology" to monitor and reconstruct environmental and climate changes has increased significantly (Weijers et al., 2012; Myers-Smith et al., 2015a; Pellizzari et al., 2017; Shetti, 2018). Given sufficient water resources, the increase in winter temperatures may promote shrub growth and richness (Franklin, 2013). Snow cover plays a key role in shrub expansion, with deeper snow having a significant positive effect on shrub growth (Holtmeier, 2003). Winter snowfall determines the start time of phenology at high latitudes and the degree of heat in early spring. Snowpack is beneficial to shrubs, which may partly explain their expansion in the Arctic in recent decades (Bjorkman et al., 2015). This in turn may lead to biophysical feedback, including regional warming and permafrost thawing (Blok et al., 2010).

Understanding how shrub growth responds to temperature changes along latitudinal gradients is crucial to accurately predict the dynamic changes of boreal forest ecosystems. However, representative data on long-term growth trend in shrubs and their climate drivers are still lacking. In addition, little is known about the growth-climate relationships of shrubs along latitudinal gradients, or about their different responses to global warming. We hypothesize that temperature plays a critical role in influencing the radial growth of shrubs at higher latitudes, whereas precipitation plays a stronger role at lower latitudes. In this study, we conduct a dendroclimatic investigation on a dominant boreal shrub species, *Pinus pumila*, along the latitudinal gradient spanning 44°–52° N in northeast China. The purpose of this study is: (1) to explore the radial growth characteristics of *P. pumila* along the latitudinal gradient, (2) to investigate changes in the growth-climate relationship of *P. pumila* along the latitudinal gradient, and (3) to evaluate potential changes in the growth of *P. pumila* in boreal forests of northeast China.

2 Materials and methods

2.1 Study area and climate data

The study area is located in northeastern China. It can be divided into three regions along the latitudinal gradient: south (44.10°–47.22° N, 120.28°–128.48° E), central (51.30°–51.62° N, 120.82°–123.53° E), and north (51.83°–52.59° N, 121.10°–123.52° E) (Table 1, Figure 1). From 2015 to 2018, we conducted field work at 12 sites, which we divided into three regions according to latitude: the southern sites (LBS, TS, AES), the central sites (DBS, ME, HM, YK, XBS), and the northern sites (AK, FKS, YA, ZL) (Table 1, Figure 1). The mean annual total precipitation (1950–2014) in the study area ranges from 415.6 to 636.2 mm (Figure 1A). The mean annual temperature is between −6.3 and 0.5°C. January and July are the coldest (−38.2°C, ZL) and hottest (25.3°C, TS) months, respectively (Table 2).

In the study area, *P. pumila* and other plant species form two main plant communities: the subalpine *Empetrum nigrum-P. pumila* community at elevations greater than 1,350 m a.s.l and the *Alnus mandshurica-P. pumila* community at elevations between 1,250 and 1,450 m a.s.l. The former is mainly distributed along flat mountain tops above 1,350 m, on open ridges, gravel heaps and the tops of mountains. The trunk of *P. pumila* creeps along the ground, with the crown rising obliquely to a height of about 1 meter. Growth is relatively weak and sparse, with 700–900 trees (clusters) per hectare. The main companion species include *Juniperus sibirica*, *Betula rotundifolia*, *Rhododendron dauricum*, *Larix gmelinii*, *Empetrum nigrum* var. *japonicum*, *Vaccinium vitis-idaea*, *Cladonia alpestris*, *Sphagnum cymbifolium*, and *Hylocomium splendens*. The latter grows under the canopy of boreal trees (Okuda et al., 2008). *Alnus mandshurica* grows vigorously and densely among *P. pumila*. The ground cover is composed mainly of *Sphagnum girgensohnii*, *Vaccinium vitis-idaea*, *Ledum palustre* var. *angustum*, *Pyrola incarnata*, etc. At high elevations, *P. pumila* usually grows between stones, while at lower altitudes, *P. pumila* grows in brown coniferous forest soil that contains a lot of sand and gravel. The sand content is 30–85%, and the gravel content greater than 2 mm is 3–35%. Although the organic matter content of brown coniferous forest soil is high, the content of nitrogen and phosphorus is low, and the ratio of carbon to nitrogen is high.

TABLE 1 Characteristics of the 12 study sites with the name of the mountain, the sample code and sample number, longitude and latitude of site, altitude of plots above sea level, and divided region.

| Site	Code	Longitude (E)	Latitude (N)	Altitude (m a.s.l.)	Sample number	Region
Laobai mountain	LBS	128° 03′	44° 06′	1,685	35	South
Tao mountain	TS	128° 29′	46° 38′	1,369	31	South
A'er mountain	AES	120° 17′	47° 13′	1,164	52	South
Dabai mountain	DBS	123° 08′	51° 18′	1,431	28	Central
Mo'erdaoga	ME	120° 49′	51° 22′	1,072	33	Central
Hanma	HM	122° 24′	51° 31′	1,000	58	Central
Yikesama	YK	121° 14′	51° 32′	1,262	36	Central
Xiaobai mountain	XBS	123° 32′	51° 37′	1,400	33	Central
Aokelidui mountain	AK	122° 03′	51° 50′	1,104	30	North
Fuke mountain	FKS	121° 40′	52° 28′	1,096	30	North
Yong'an	YA	121° 06′	52° 33′	1,196	60	North
Zhalinku'er	ZL	123° 31′	52° 35′	1,135	58	North
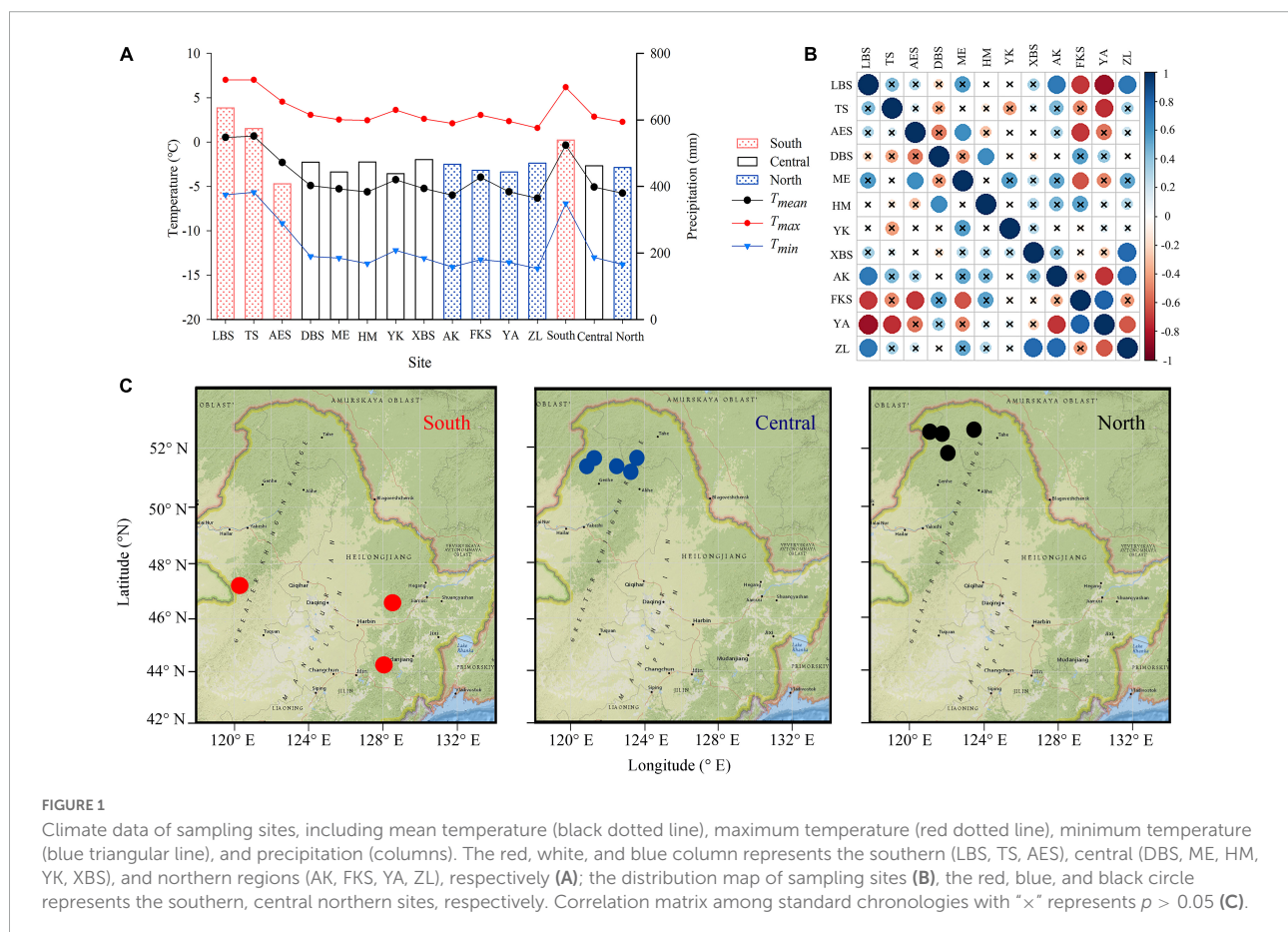
FIGURE 1
Climate data of sampling sites, including mean temperature (black dotted line), maximum temperature (red dotted line), minimum temperature (blue triangular line), and precipitation (columns). The red, white, and blue column represents the southern (LBS, TS, AES), central (DBS, ME, HM, YK, XBS), and northern regions (AK, FKS, YA, ZL), respectively **(A)**; the distribution map of sampling sites **(B)**, the red, blue, and black circle represents the southern, central northern sites, respectively. Correlation matrix among standard chronologies with "×" represents $p > 0.05$ **(C)**.

Because there are no weather stations nearby, we used the monthly and seasonal temperature and precipitation data of the CRU TS 4.04 0.5° × 0.5° grid to analyze the growth-climate relationships from 1950 to 2014. The data were extracted from the sampling area using the KNMI Climate Explorer web page.[1] The CRU database is formed by interpolating data from regional meteorological stations. Climate variables

---

1 http://climexp.knmi.nl

TABLE 2 Major characteristics of standard chronologies (STD) chronologies in 12 sites *Pinus pumila* in northeast China, mean ring width, chronology time span, mean sensitivity (MS), standard deviation (SD), signal-to-noise ratio (SNR), mean intercorrelation between individual series inter-series correlation (R_{bar}), autocorrelation of order 1 (AC1), variance in the first eigenvector (%) (VF1), and expressed population signal (EPS) included in in the dendroecological network.

Site	Mean ring width (mm)	Chronology time span	MS	SD	ACI	VF1%	R_{bar}	EPS	SNR
LBS	0.52	1937–2017	0.14	0.29	0.84	27.22	0.18	0.89	8.09
TS	0.27	1907–2017	0.12	0.22	0.80	19.61	0.10	0.80	3.87
AES	0.44	1934–2017	0.15	0.16	0.40	23.52	0.1	0.79	3.83
DBS	0.65	1945–2014	0.14	0.19	0.56	26.82	0.16	0.85	4.42
ME	0.53	1867–2017	0.22	0.28	0.45	28.05	0.15	0.85	4.24
HM	0.43	1891–2018	0.17	0.21	0.46	26.98	0.22	0.94	14.81
YK	0.55	1923–2017	0.17	0.21	0.87	21.44	0.16	0.85	6.70
XBS	0.52	1946–2014	0.14	0.16	0.38	24.50	0.21	0.92	12.15
AK	0.50	1943–2014	0.15	0.32	0.81	37.92	0.27	0.89	8.27
FKS	0.39	1881–2014	0.17	0.23	0.62	24.76	0.19	0.87	6.66
YA	0.49	1903–2017	0.13	0.17	0.55	27.14	0.22	0.90	9.43
ZL	0.49	1949–2017	0.19	0.23	0.54	29.49	0.24	0.92	10.75

FIGURE 2
Standard chronologies of different regions **(A,B)**. Violin plot shows the full distribution of data, with white dots referring to the median, and colored dots describing mean shrub-ring width in different regions **(C)**. The range of the black lines in the violins represents the interquartile ranges, and the light bar represents the 95% confidence interval. "**" and "*" represents $p < 0.01$ and $p < 0.05$, respectively.

for growth-climate response analysis include monthly total precipitation (P) and mean (T_{mean}), minimum (T_{min}), and maximum temperature (T_{max}) (**Figure 2**). We define winter as from December of the previous year to February of the current year, spring as from March to May, summer as from June to August, and autumn as from September to November.

2.2 Dendrochronological sampling, treatment, and analysis

At each site, 10–15 discs of *P. pumila* were cut with a handsaw. These samples were obtained only from isolated,

mature, and healthy individuals to avoid competition with other plants that may affect stem growth. A total of 140 discs from 12 sites (**Figure 1**, **Table 1**) were sampled along the latitudinal gradient from south to north. The cross-section of each disc was naturally air-dried and polished with increasingly fine grades of sandpaper (120–800 grit) until the ring boundary could be clearly distinguished under a microscope (Fritts, 1976; Cook and Kairiukstis, 1990). The rings of *P. pumila* were cross-dated and ring widths were measured in the laboratory using traditional dendrochronological methods (Fritts, 1976; Cook and Kairiukstis, 1990). Two to four radii in each disc were cross-dated, and the ring width at each radius direction was measured using the Velmex measurement system with a resolution of 0.001 mm. The cross-dating and measurement accuracy

were statistically checked using the COFECHA computer program (Holmes, 1983), which determined the degree of synchronization between series according to the correlation with the main chronology.

Each ring-width series was detrended and standardized by fitting a negative exponential curve or linear line using the ARSTAN program to remove non-climate signals related to age or stand dynamic effects (Cook and Holmes, 1986). The ring-width index was obtained by dividing the ring width by the fitting value of each ring. Three kinds of ring-width chronologies (standard, residual, and autoregression chronologies) were obtained by averaging all detrended series with a bi-weight robust mean (Cook and Kairiukstis, 1990). Raw measured ring widths and the standard chronologies (STD) were used in the subsequent analyses.

Chronology parameters are statistical using the ARSTAN program. The expressed population signal (EPS), defined as the proportion of each series signal of the total series variance, was used to quantify the reliability of the chronology (Wigley et al., 1984). The mean sensitivity (MS) and the first order autocorrelation (AC1) were calculated on the individual detrended index series, then averaged to measure the year-to-year variability and the degree to which current-year growth was influenced by previous-year climate factors. The mean series correlation between trees (R_{bar}) allows us to evaluate the strength of the common growth signal over time. The standard deviation (SD) of inter-annual ring-width variability was calculated as a proportion of mean ring-width (Chen et al., 2011). Variance in the first eigenvector (VF1) of all series identifies the common growth variability among all trees at each site. The signal-to noise ratio (SNR) is a measure of the strength of the common high-frequency signal in the ring-width indices of trees from the same site.

2.3 Climate−growth relationship analysis

Pearson correlation was used to analyze the relationship between the chronology and monthly and seasonal climate variables to compare the climate factors limiting radial growth in different regions. The climatic factors from May to October of the previous year were selected for analysis because the climate of the previous and current year affects the radial growth of trees in the current year (Fritts, 1976). We also carried out correlation analyses for two periods (1950–1980 and 1981–2014) to investigate the impact of recent rapid warming (after 1980) on the growth of *P. pumila*.

The responses of *P. pumila* individuals to temperature were categorized as one of four response patterns: positive (more than 67% of individuals at a site are significantly positively correlated with temperature), negative (less than 33% are significantly positively correlated with temperature), mixed (between 33 and

67% are significantly positively correlated with temperature), or none (no significant correlation with temperature) (Lloyd et al., 2011). The response patterns of *P. pumila* to precipitation were similarly classified, and the proportion of shrubs exhibiting each response pattern was tallied for each site. Then, linear mixed-effects models (LMEs) were used to identify the effects of eight climate variables (T_{wi}: temperature in winter, T_{sp}: temperature in spring, T_{su}: temperature in summer, T_{au}: temperature in autumn, P_{wi}: precipitation in winter, P_{sp}: precipitation in spring, P_{su}: precipitation in summer, and P_{au}: precipitation in autumn) on the residuals of the previous function. Climate variables during 1950–2014 were used as fixed factors, while individual shrubs were considered random factors. Fitted models follow the equation:

$$RW_i = Xa_i + Zb + e_i,$$

where RW_i represents the ring width at year i; a is the vector of fixed factors (seasonal climate variables), b is the vector of random factors (shrub identity), X and Z are the fixed and random effects regressor matrices, respectively, and ei is the within-group error vector (Camarero et al., 2017). We ranked all the potential models that could be generated with the different explanatory variables according to the Akaike information criterion (AIC). We chose the most parsimonious models; that is, the models with the lowest AICs (Burnham and Anderson, 2002). For each site, the model with the lowest number of variables among those with the lowest AIC was selected as the final model (Burnham and Anderson, 2002). In addition, we used the Akaike weights (Wi) of each model to measure the conditional probability of the candidate model, assuming it was the best model. By using seasonal climate averages instead of monthly data, we can create more parsimonious models while maintaining a reliable representation of climate trends (Matías et al., 2017). The linear mixed model analysis was performed using the LME4 package in R 4.0.3 (R Core Team, 2015). Hierarchical cluster analysis and correlation analysis were performed using the SPSS 18.0 software package (IBM SPSS Inc., Chicago, IL, USA). Finally, the ring-width growth trend of *P. pumila* under four emission scenarios (RCP 2.6, RCP 4.5, RCP 6.0, and RCP 8.5) was simulated through the linear regression prediction under the CMIP5 scenarios of 2020–2100 predicted by HadGEM2-ES.

3 Results

3.1 Comparison of chronological characteristics and growth trends

The mean age of shrubs at the 12 sites ranges from 69 to 151 years, and the mean ring width varies from 0.27 to 0.65 mm (Table 2). ME has the highest MS, AK has the highest SD, VF1 and R_{bar}, YK has the highest AC1, and HM has the highest

EPS and SNR (**Table 2**). In short, the chronological statistics of *P. pumila* at different sites show significant trends. All analyses indicate that the 12 chronologies have abundant climate signals and are suitable for analyzing growth-climate relationships. The Pearson correlations analysis result shows a high correlation among sites in the same region (**Figure 1C**). From 1950 to 1980, the ring-width index of *P. pumila* increased significantly in the south and central regions, but did not increase significantly in the northern region. After 1980, the chronology trends diverge in different regions, with the southern and central regions showing a slight downward trend, and the northern region showing an upward trend (**Figure 2A**). There is no significant difference in ring width between different regions (**Figure 2B**).

3.2 Responses of shrub radial growth to climate factors

The chronology of *P. pumila* in the north is significantly positively correlated with temperature in January and May (**Figures 3A–C**). Warm winter conditions enhance the growth of *P. pumila* in the north and south (**Figures 3A–C**). In addition, wet winter conditions are positively correlated with the growth of *P. pumila* in the north. The ring widths of *P. pumila* are significantly correlated with minimum temperature from April to June, especially in the north. Wet conditions in June promote the growth of *P. pumila* in all three regions. It should be noted that there is no significant correlation between the growth of *P. pumila* and monthly maximum temperature in summer. However, warm autumn conditions are conducive to the growth of *P. pumila* in the north and south. Temperature during the previous growing season has a positive effect on the radial growth of *P. pumila*. The results show that the growth response of *P. pumila* varies with latitude, and that each region has at least three different response classes (**Figure 3**).

Northern *P. pumila* individuals respond more negatively to temperature than their southern and central counterparts, but many individuals exhibit a positive relationship with temperature (**Figure 4**). Moreover, *P. pumila* individuals that are positively correlated with temperature show more growth in colder years (**Figure 4A**).

3.3 Responses of shrub growth to seasonal climate factors at different periods

During the period 1950–1980, the growth of *P. pumila* was negatively correlated with summer temperature, positively correlated with winter temperature, and positively correlated with summer and winter precipitation (**Figure 5**). However, from 1981 to 2014, the growth of *P. pumila* was positively correlated with summer temperature and negatively correlated

with winter temperature with increasing latitude (**Figure 5**). This may be due to the higher winter temperature growth rates at high latitudes from 1981–2014. In the more recent 30-year period, the correlation between the growth of *P. pumila* and summer precipitation decreased with increasing latitude, while the correlation between the growth of *P. pumila* and winter precipitation increased (**Figures 4**, **5**).

3.4 Growth prediction of *P. pumila* under different climate change scenarios

We developed a prediction model for the relationship between the growth of *P. pumila* and the main climate factors. For the climate change predicted by the HadGEM2-ES RCP 2.6 scenario, our model predicts that the growth of *P. pumila* in the central region will stabilize before 2100 (**Table 3**, **Figure 6**). In contrast, the growth of *P. pumila* increases slightly in the south and decreases slightly in the north. Under the RCP 4.5 and RCP 6.0 scenarios, the growth of *P. pumila* in the south increases rapidly. Under the RCP 8.5 scenario, the growth of *P. pumila* in the south increases rapidly until 2100 (**Figure 6**). In contrast, the growth of *P. pumila* in the northern and central regions shows a downward trend in the RCP 4.5, RCP 6.0, and RCP 8.5 scenarios (**Figure 6**).

4 Discussion

4.1 The main climate factors limiting *P. pumila* growth at different latitudes

The growth of *P. pumila* in the south is limited by temperature during the growing season. This might be because the average elevation of the southern sampling sites (1,310 m) is higher than that of the central and northern sites; average annual precipitation is also greater (Li et al., 2020). Therefore, moisture is not the main factor limiting the growth of *P. pumila* in the southern part of the study area. The increase in winter temperature of the previous year promotes the growth of *P. pumila* in the southern and northern regions but has little impact on the growth of *P. pumila* in the central region. High temperatures in winter accelerate snow melting, providing sufficient water supply during the subsequent growing season and enhancing radial growth rates (Duan et al., 2017; Lyu et al., 2017). In addition, warm winters help protect needles and fine roots from frost damage (Myers-Smith et al., 2011; Duan et al., 2017). The timing of soil thaw plays a crucial role in initiating the physiological activity of shrubs (Vaganov et al., 1999; Kirdyanov et al., 2003; Lloyd et al., 2011). Therefore, winter warming may be beneficial to the growth of high-altitude shrubs.
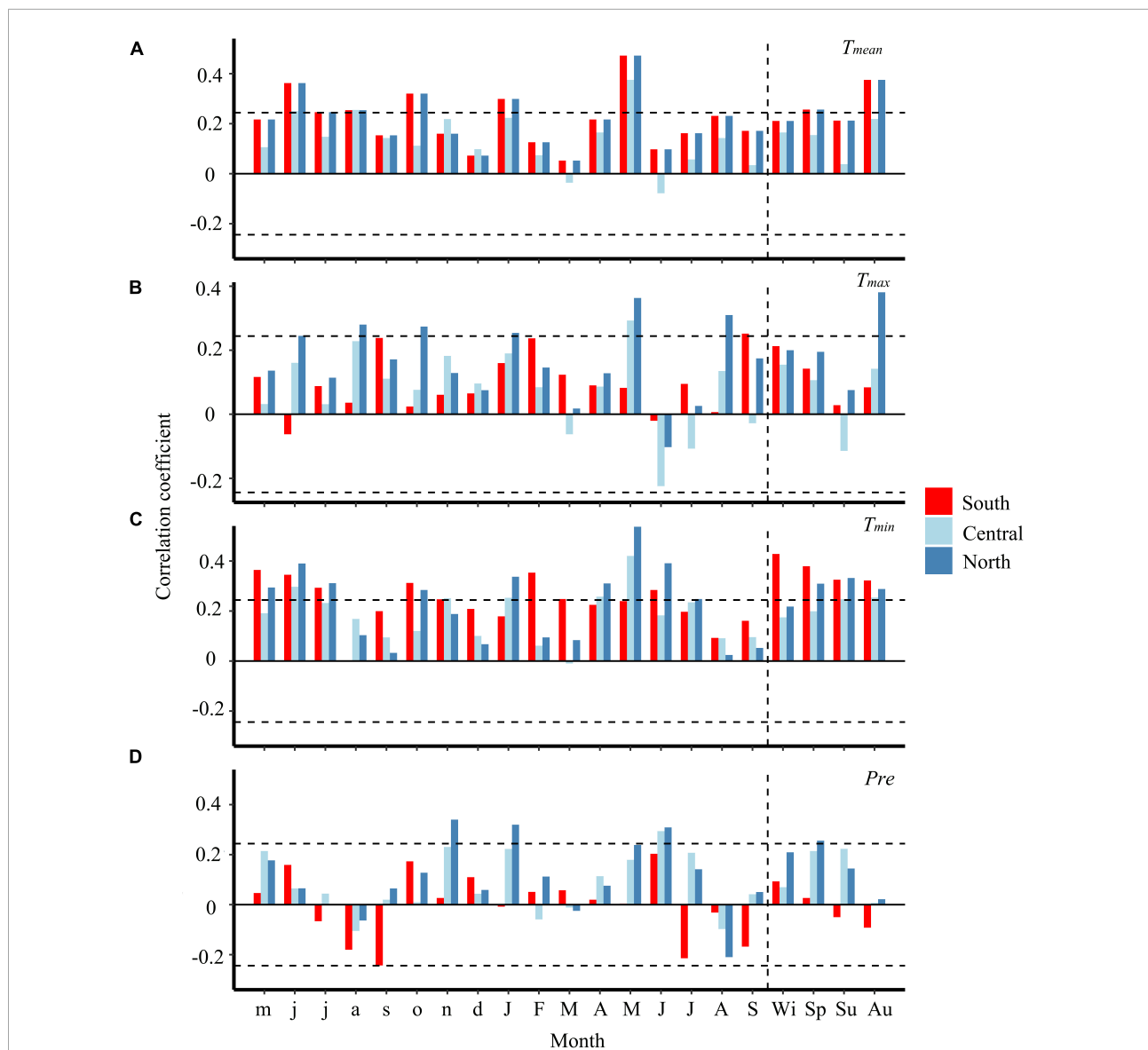
FIGURE 3
Correlation between regional chronologies and monthly climate factors from 1950 to 2014. Climate parameters include monthly mean temperature **(A)**, maximum temperature **(B)**, minimum temperature **(C)**, and monthly total precipitation **(D)**. Horizontal dash line represents the significance at $p < 0.05$. Lowercase and uppercase letters on the axis indicate the month of the previous year and the current year. Wi, Sp, Su, and Au represent the prior winter, current spring, summer, and autumn, respectively.

The sensitivity of *P. pumila* growth to temperature varies along the latitudinal gradient. The positive correlations between *P. pumila* growth and minimum temperature highlight the importance of winter and spring temperatures in the north (**Figure 4**). Frost may affect shrub growth at high latitudes before the growing season (Li et al., 2020). In a cold environment, spring temperatures and the length of the growing season are important factors limiting the production and differentiation of xylem cells (Morales et al., 2012; Lenz et al., 2013; Yang et al., 2020). Higher temperatures in early spring may favor coniferous species because their evergreen leaves enable them

to take advantage of early warmth (Jiang et al., 2016). Myers-Smith et al. (2011) found a significant positive correlation between the ring widths of some of the most common shrub species in the tundra ecosystem and the mean growing season temperature. However, winter and spring temperatures seem less critical to the growth of *P. pumila* in the central region as compared to the northern and southern regions. The impact of maximum summer temperature on the growth of *P. pumila* is not significant, suggesting that the initial climate conditions of the growing season are more important for a positive growth response (**Figure 4**). However, we found that high temperature
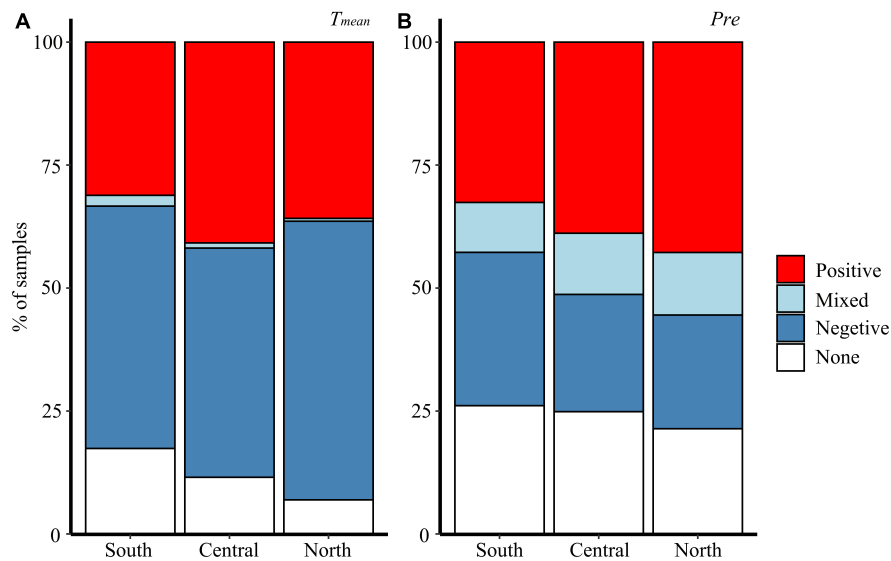
FIGURE 4
Response pattern to mean temperature **(A)** and precipitation **(B)**. Response categories are defined in the Methods. Bars indicate the percent of *P. pumila* at each region in each response category. The site is arranged from the southernmost (LBS) to the northernmost (ZL).
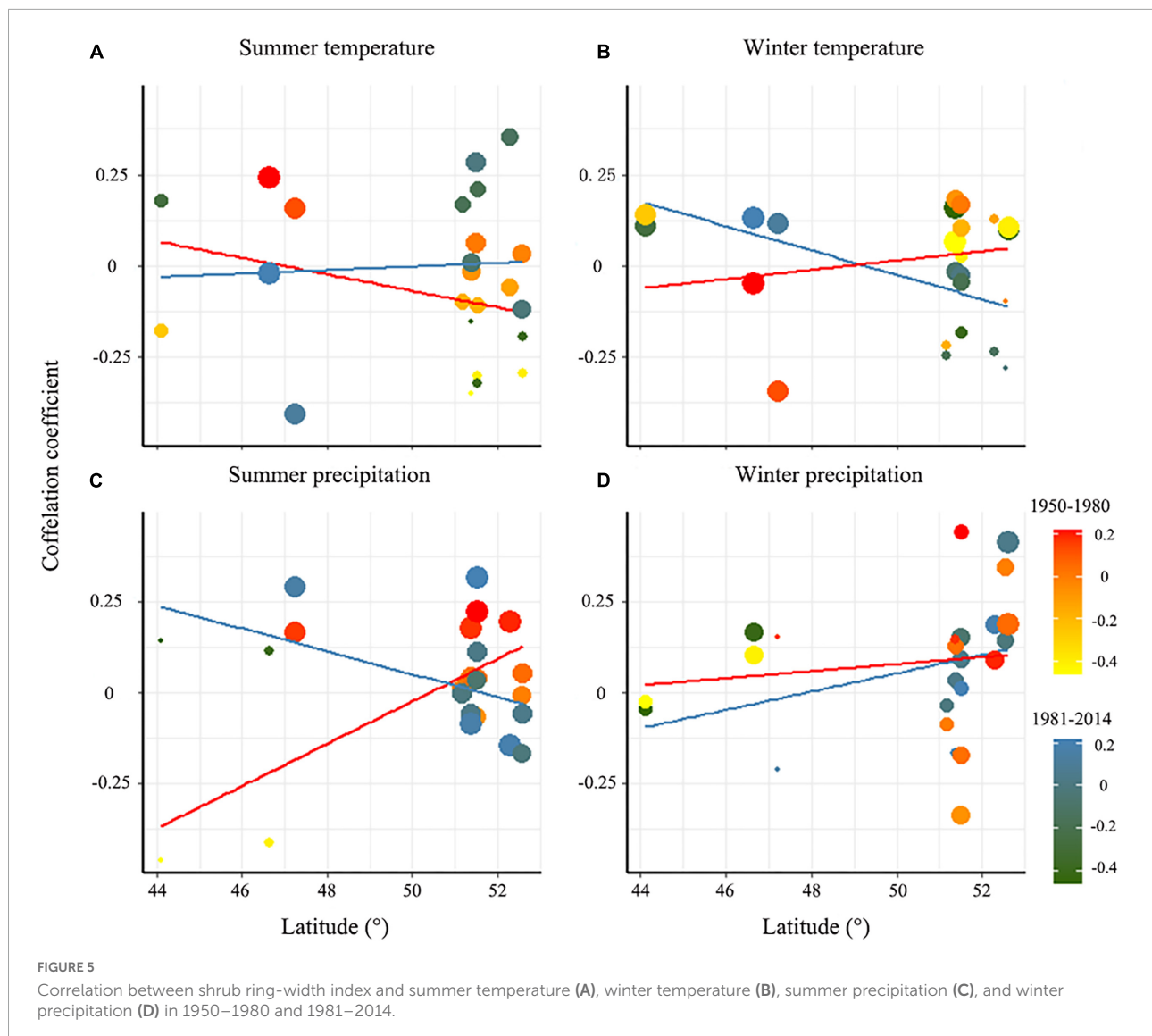
and insufficient water in summer still has a negative impact on the growth of *P. pumila* (Yang et al., 2020).

At the individual level, the responses of *P. pumila* growth to precipitation are consistent, with precipitation more strongly influencing growth in the northern areas. The more northward *P. pumila* grows, the more negative its growth response to temperature is. This is inconsistent with the results of previous studies, which show a pattern of more positive responses to warming in northern region (Lloyd et al., 2011). However, we found that more than half of the northern *P. pumila* individuals have a negative response to temperature, which may be caused by the synchronous constraining effects of hydrothermal coupling on the growth of *P. pumila* (Yang et al., 2020). Individual shrubs differ in many respects, including size, age, microsite conditions, competition, and genome (Huebner and Bret-Harte, 2019). The population-based approach emphasizes the mean climate signal, but the cost is the loss of individual-level information (Galván et al., 2014). Thus, although population chronology can highlight regional climate information, it may bias subsequent inferences. This is especially true for dwarf shrubs growing in harsh environments (Sedlacek et al., 2016), as each shrub individual may experience different microenvironment conditions. The difference between individuals in the population is the reality of nature, whereas the mean value is a statistical abstraction (Carrer, 2011). However, Bär et al. (2008) found that while the topoclimate at different microsites leads to slight changes in the annual growth pattern of *Emperum hermaloditum*, the prominent regional climate signals are still reflected in shrub growth at all microsites.

The altitude and longitude that cause environmental heterogeneity may also affect the growth and physiology of shrubs (McDowell and Sevanto, 2010). High-altitude shrubs are more limited by low temperatures, whereas low-altitude shrubs are more limited by water (Lu et al., 2021). The precipitation difference caused by longitude also affects the relationship between shrub growth and climate factors and may further affect their responses to drought and warming (Li et al., 2016; Anderegg et al., 2019; Buchwal et al., 2020). Therefore, our results may include the combined effects of latitude, longitude, and elevation on shrub growth.

4.2 Differences and similarities in the responses of *P. pumila* at different latitudes to rapid warming after 1980

From 1950 to 1980, the radial growth of *P. pumila* is limited by moisture deficits in summer and low winter temperatures. However, the growth of *P. pumila* in the northern region is more susceptible to winter precipitation from 1981 to 2014 due to climate warming. The weakening of temperature seasonality in the Northern Hemisphere due to anthropogenic forcing, as well as future human impacts, may further weaken the annual temperature cycle, thereby affecting biological and ecological systems, especially at high latitudes (50°–70 °N) (Rosenzweig et al., 2008; Qian and Zhang, 2015; Duan et al., 2017). The degree of warming in northern China over the past 60 years has exceeded that of southern China (Xu et al., 2021). Seasonal warming during the 1958–2017 period was highest in winter

FIGURE 5
Correlation between shrub ring-width index and summer temperature **(A)**, winter temperature **(B)**, summer precipitation **(C)**, and winter precipitation **(D)** in 1950–1980 and 1981–2014.

and lowest in summer (Xu et al., 2021). Winter warming has exceeded summer warming since the end of 19th century, and the magnitude of the annual temperature cycle has decreased by 0.45°C/100 a (Duan et al., 2017). The rapid warming since 1980, particularly in winter, will affect the radial growth of *P. pumila,* with a more pronounced influence at higher latitudes (increased drought). If warming continues, water stress may become the main factor limiting the growth of *P. pumila* in the future.

4.3 Prediction of *P. pumila* growth in different regions under future climate change scenarios

The growth of *P. pumila* in the north shows an unexpected but clear downtrend under the climate warming scenario,

whereas growth in the south shows an upward trend. The relationship between climate factors and *P. pumila* growth is not perfectly linear due to the influence of multiple climate factors (Shao et al., 2021; Zheng et al., 2021). In addition, climate also compensates the radial growth of trees or shrubs (Jiang et al., 2015; Cao et al., 2016). The model results may be affected by the linear relationship between climate factors and shrub growth (Bonan, 2008). Many studies have confirmed that shrub growth increases and expands to higher latitudes (Myers-Smith et al., 2015b; Myers-Smith et al., 2020) as global warming leads to extended growing seasons (Huang et al., 2011; Rossi et al., 2016). Compared with shrubs, the proportion of trees (larch and pine) threatened by high summer temperatures will increase by 45.5 to 63.6% (Li et al., 2020). In our study area, the degradation of permafrost due to the increase in ground surface temperature has led to a rapid increase in the growth

TABLE 3 Best linear mixed models explaining the effect of climate on ring width after accounting for seasonal climate factor effects for the different regions across the latitudinal gradients.

Latitude	Growth model	K	AIC	△AIC	*Wi*
South	$T_{wi} + T_{sp} + P_{su}$	5	−140.5	0	0.99
	$T_{wi} + T_{sp} + T_{su} + T_{au} + P_{su}$	7	−128.8	11.7	0
	$T_{wi} + T_{sp} + T_{su} + P_{sp} + P_{su}$	7	−127.0	13.5	0
	$T_{wi} + T_{au} + T_{sp} + T_{su} + T_{sp} + P_{su}$	8	−117.8	22.7	0
	$T_{wi} + T_{sp} + T_{su} + T_{au} + P_{sp} + P_{su} + P_{wi}$	9	−108.2	32.3	0
	$T_{wi} + T_{sp} + T_{su} + T_{au} + P_{sp} + P_{su} + P_{au} + P_{wi}$	10	−94.5	46.0	0
Central	$T_{wi} + T_{su} + T_{au} + P_{sp}$	6	−125.4	0	0.99
	$T_{wi} + T_{sp} + T_{au} + P_{sp} + P_{su}$	7	−111.2	14.2	0
	$T_{wi} + T_{su} + T_{au} + P_{sp} + P_{su}$	7	−109.8	15.6	0
	$T_{wi} + T_{au} + T_{su} + P_{wi} + P_{su} + P_{au}$	8	−95.1	30.2	0
	$T_{wi} + T_{sp} + T_{su} + T_{au} + P_{wi} + P_{au} + P_{su}$	9	−89.3	36.1	0
	$T_{wi} + T_{sp} + T_{su} + T_{au} + P_{wi} + P_{sp} + P_{su} + P_{au}$	10	−79.2	46.2	0
North	$T_{wi} + T_{sp} + T_{au} + P_{wi} + P_{sp}$	7	−58.1	0	0.87
	$T_{wi} + T_{sp} + T_{su} + P_{wi} + P_{sp}$	7	−54.1	4.0	0.12
	$T_{wi} + T_{sp} + T_{su} + T_{au} + P_{wi} + P_{sp}$	8	−50.1	8.0	0.01
	$T_{wi} + T_{sp} + T_{su} + T_{au} + P_{wi} + P_{sp} + P_{au}$	9	−36.9	21.1	0
	$T_{wi} + T_{sp} + T_{su} + T_{au} + P_{wi} + P_{sp} + P_{su}$	9	−36.8	21.3	0
	$T_{wi} + T_{sp} + T_{su} + T_{au} + P_{wi} + P_{sp} + P_{su} + P_{au}$	10	−23.6	34.4	0

Selected models are highlighted in bold. The best models were selected based on the Akaike information criteria (AIC). K represents the number of variables included in the model plus constant and error terms, △AIC is the difference in AIC respect the best model, and *Wi* is the relative probability to be the best model for the observed data. T_{wi}, T_{sp}, T_{su}, and T_{au} are the temperature in winter of the previous year and in spring, summer, and autumn of the current year, respectively. Similar names for precipitation values (P_{wi}, P_{sp}, P_{su}, and P_{au}).
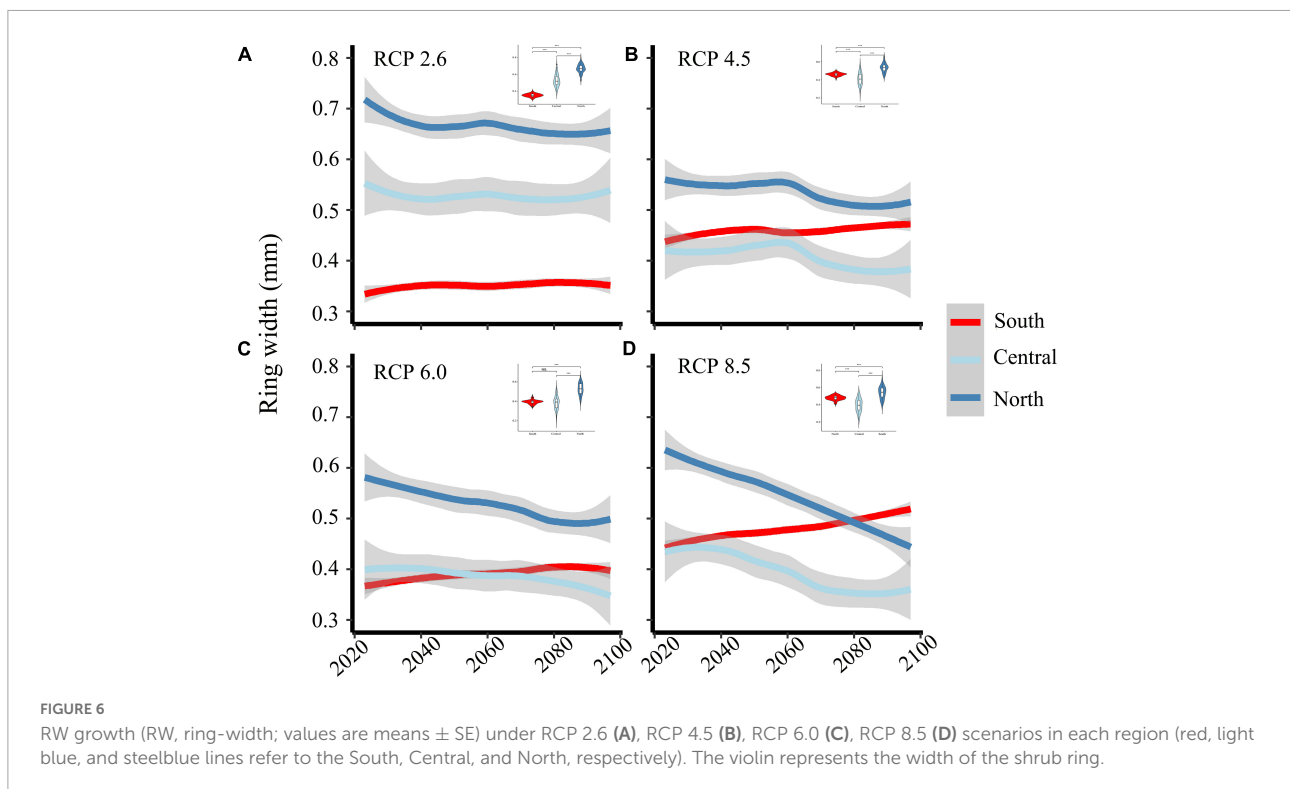

FIGURE 6
RW growth (RW, ring-width; values are means ± SE) under RCP 2.6 **(A)**, RCP 4.5 **(B)**, RCP 6.0 **(C)**, RCP 8.5 **(D)** scenarios in each region (red, light blue, and steelblue lines refer to the South, Central, and North, respectively). The violin represents the width of the shrub ring.

of larch in the past decade (Zhang et al., 2019). However, the impact of soil warming on the growth of *P. pumila*, which has a shallow root system, remains unclear. Under different scenarios of HadGEM2-ES, the growth of *P. pumila* in the south exhibits an increasing trend until 2100 (**Figure 6**). In contrast, the growth of *P. pumila* in the northern and central regions decreases slightly or shows a steady trend (**Figure 6**). Under the future warming scenario, the growth of *P. pumila* in the northern and central regions will be significantly reduced. This is mainly because water plays an important role in shrub growth in these regions. When there is sufficient moisture, shrub growth benefits from the continuous warming (Myers-Smith et al., 2015a). Therefore, in areas where trees are sensitive to warming and drought due to rising temperatures, shrubs may become the dominant plant life form. In these areas, even if shrubs gradually replace trees, it will take a long time. Conversely, changes in shrub distribution and coverage may also have a feedback impact on climate change (Myers-Smith et al., 2011).

5 Conclusion

Continuous warming may have a greater impact on the growth of *P. pumila* in the northern part of northeast China than in more southern regions. Warming that precedes the growing season (the winter of the previous year and the spring of the current year) promotes the growth of *P. pumila* in the southern and northern extents of its distribution. Increasing maximum summer temperatures have had little effect on the growth of *P. pumila* across the latitudinal gradient. At the individual level, the increase in precipitation has promoted the growth of *P. pumila* in the northern region of the study area, while the increase in temperature has inhibited growth. The LMEs predict that the growth of *P. pumila* in the northern part of northeast China will decrease slightly under the RCP2.6 scenario. In contrast, under the RCP4.5, RCP6.0, and RCP8.5 scenarios, the growth of *P. pumila* in the south will increase. Therefore, the growth response of *P. pumila* to warming varies along the latitudinal gradient, and depends mainly on the water status of the region. As the dominant shrub species in boreal forests, *P. pumila* may not expand northward (because the northern region is drier than the southern region) under a warming climate, and is likely to replace the native tree species in some areas. We recommend that future research focus on how individual shrubs respond to changing climate conditions, as this information is crucial for predicting dynamic changes in shrub growth and distribution. Shrubs help to conserve water, reduce erosion, improve soil, and provide food and shelter for small animals. The proper management of boreal forest shrubs in the context of a warming climate is important for safeguarding these important ecosystem services.

Data availability statement

The raw data supporting the conclusions of this article will be made available by the authors, without undue reservation.

Author contributions

JY and XW conceived the study. JY, QZ, WS, and XW designed the field sampling. JY, YA, and WS collected the field samples and data. JY undertook all lab work and data analyses and wrote the first draft of the manuscript. All authors revised the manuscript.

Funding

Acknowledgments

Conflict of interest

The authors declare that the research was conducted in the absence of any commercial or financial relationships that could be construed as a potential conflict of interest.

Publisher's note

All claims expressed in this article are solely those of the authors and do not necessarily represent those of their affiliated organizations, or those of the publisher, the editors and the reviewers. Any product that may be evaluated in this article, or claim that may be made by its manufacturer, is not guaranteed or endorsed by the publisher.

References

Anderegg, W. R., Anderegg, L. D., and Huang, C. Y. (2019). Testing early warning metrics for drought–induced tree physiological stress and mortality. *Glob. Chang. Biol.* 25, 2459–2469. doi: 10.1111/gcb.14655

Bär, A., Pape, R., Bräuning, A., and Löffler, J. (2008). Growth-ring variations of dwarf shrubs reflect regional climate signals in alpine environments rather than topoclimatic differences. *J. Biogeogr.* 35, 625–636. doi: 10.1111/j.1365-2699.2007.01804.x

Bjorkman, A. D., Elmendorf, S. C., Beamish, A. L., Velend, M., and Gregory, H. R. H. (2015). Contrasting effects of warming and increased snowfall on *Arctic tundra* plant phenology over the past two decades. *Glob. Chang. Biol.* 21, 4651–4661. doi: 10.1111/gcb.13051

Blok, D., Heijmans, M. M. P. D., Schaepman-strub, G., Kononov, A. V., Maximov, T. C., and Berendse, F. (2010). Shrub expansion may reduce summer permafrost thaw in Siberian tundra. *Glob. Chang. Biol.* 16, 1296–1305. doi: 10.1111/j.1365-2486.2009.02110.x

Bonan, G. B. (2008). Forests and climate change: Forcings, feedbacks, and the climate benefits of forests. *Science* 320, 1444–1449. doi: 10.1126/science.1155121

Buchwal, A., Sullivan, P. F., Macias-Fauria, M., Post, E., Myers-Smith, I. H., Stroeve, J. C., et al. (2020). Divergence of Arctic shrub growth associated with sea ice decline. *PNAS* 117, 33334–33344. doi: 10.1073/pnas.2013311117

Burnham, K. P., and Anderson, D. R. (2002). *Model Selection and Multimodel Inference: A Practical Information-Theoretic Approach*. Heidelberg: Springer.

Camarero, J. J., Linares, J. C., García-Cervigón, A. I., Batllori, E., Martínez, I., and Gutiérrez, E. (2017). Back to the future: The responses of alpine treelines to climate warming are constrained by the current ecotone structure. *Ecosystems* 20, 683–700. doi: 10.1007/s10021-016-0046-3

Cao, C. F., Zhou, F. F., Dong, Z. P., Li, Y. J., Zhang, Y., Li, D. W., et al. (2016). Study on nonlinear climate growth patterns of Pinus taiwanens in Daiyun Mountain. Fujian Province. *J. Subtrop. Res. Environ.* 11, 44–51.

Carrer, M. (2011). Individualistic and time–varying tree–ring growth to climate sensitivity. *PLoS One* 6:e22813. doi: 10.1371/journal.pone.0022813

Chen, L., Wu, S., and Pan, T. (2011). Variability of climate-growth relationships along an elevation gradient in the Changbai Mountain, northeastern China. *Trees* 25, 1133–1139. doi: 10.1007/s00468-011-0588-0

Cook, E. R., and Holmes, R. L. (1986). *User's manual for program ARSTAN*. Tucson, AZ: Laboratory of Tree Ring Research, University of Arizona.

Cook, E. R., and Kairiukstis, L. (1990). *Methods of dendrochronology: applications in the environmental sciences*. Dordrecht: Kulwer.

Duan, J., Esper, J., Büntgen, U., Li, J., Xoplaki, E., Zhang, H., et al. (2017). Weakening of annual temperature cycle over the Tibetan Plateau since the 1870s. *Nat. Commun.* 8:14008. doi: 10.1038/ncomms14008

Fang, J., Chen, A., Peng, C., Zhao, S., and Ci, L. (2001). Changes in forest biomass carbon storage in China between 1949 and 1998. *Science* 292, 2320–2322. doi: 10.1126/science.1058629

Fang, O., and Zhang, Q. B. (2019). Tree resilience to drought increases in the Tibetan Plateau. *Glob. Chang. Biol.* 25, 245–253. doi: 10.1111/gcb.14470

Franklin, R. S. (2013). Growth response of the alpine shrub, *Linanthus pungens*, to snowpack and temperature at a rock glacier site in the eastern Sierra Nevada of California, USA. *Quat. Int.* 310, 20–33. doi: 10.1016/j.quaint.2012.07.018

Fritts, H. (1976). *Tree rings and climate*. New York, NY: Academic Press.

Galván, J. D., Camarero, J. J., and Gutiérrez, E. (2014). Seeing the trees for the forest: Drivers of individual growth responses to climate in Pinus uncinata mountain forests. *J. Ecol.* 102, 1244–1257. doi: 10.1111/1365-2745.12268

Gauthier, S., Bernier, P., Kuuluvainen, T., Shvidenko, A. Z., and Schepaschenko, D. G. (2015). Boreal forest health and global change. *Science* 349, 819–822. doi: 10.1126/science.aaa9092

Holmes, R. L. (1983). Computer-assisted quality control in tree ring dating and measurement. *Tree Ring Bull.* 43, 69–78.

Holtmeier, F. K. (2003). *Physiognomic and ecological differentiation of mountain timberline*. Dordrecht: Springer.

Huang, J. G., Bergeron, Y., Zhai, L., and Denneler, B. (2011). Variation in intra-annual radial growth (xylem formation) of Picea mariana (Pinaceae) along

a latitudinal gradient in western Quebec. Canada. *Am. J. Bot.* 98, 792–800. doi: 10.3732/ajb.1000074

Huebner, D. C., and Bret-Harte, M. S. (2019). Microsite conditions in retrogressive thaw slumps may facilitate increased seedling recruitment in the Alaskan Low Arctic. *Ecol. Evol.* 9, 1880–1897. doi: 10.1002/ece3.4882

IPCC (2021). "Climate change 2021: The physical science basis," in *Proceedings of the Contribution of Working Group I to the Sixth Assessment Report of the Intergovernmental Panel on Climate Change*, (Geneva: IPCC).

Jiang, Y., Zhang, J., Han, S., Chen, Z., Setälä, H., Yu, J., et al. (2016). Radial growth response of Larix gmelinii to climate along a latitudinal gradient in the greater Khingan mountains, northeastern China. *Forests* 7, 295–306. doi: 10.3390/f7120295

Jiang, Y., Zhou, G., Wang, Y., Wang, H., and Shi, Y. (2015). Advances in the adaptability of zonal Stipa plants to CO2 and climate change in Inner Mongolia. *Acta. Ecol. Sinica* 35, 4559–4569. doi: 10.5846/stxb201311072691

Jump, A. S., Hunt, J. M., and Peñuelas, J. (2006). Rapid climate change–related growth decline at the southern range edge of Fagus sylvatica. *Glob. Chang. Biol.* 12, 2163–2174. doi: 10.1111/j.1365-2486.2006.01250.x

Kirdyanov, A., Hughes, M., Vaganov, E., Schweingruber, F., and Silkin, P. (2003). The importance of early summer temperature and date of snow melt for tree growth in the Siberian Subarctic. *Trees* 17, 61–69. doi: 10.1007/s00468-002-0209-z

Kueppers, L. M., Conlisk, E., Castanha, C., Andrew, B. M., Matthew, J. G., Perry, et al. (2017). Warming and provenance limit tree recruitment across and beyond the elevation range of subalpine forest. *Glob. Chang. Biol.* 23, 2383–2395. doi: 10.1111/gcb.13561

Lenz, A., Hoch, G., and Körner, C. (2013). Early season temperature controls cambial activity and total tree ring width at the alpine treeline. *Plant Ecol. Divers.* 6, 365–375.

Li, B., Heijmans, M. M. P. D., Berendse, F., Blok, D., Maximov, T., and Sass-Klaassen, U. (2016). The role of summer precipitation and summer temperature in establishment and growth of dwarf shrub Betula nana in northeast Siberian tundra. *Polar Biol.* 39, 1245–1255. doi: 10.1007/s00300-015-1847-0

Li, W., Jiang, Y., Dong, M., Du, E., Zhou, Z., Zhao, S., et al. (2020). Diverse responses of radial growth to climate across the southern part of the Asian boreal forests in northeast China. *For. Ecol. Manage.* 458:117759. doi: 10.1016/j.foreco.2019.117759

Lloyd, A. H., Bunn, A. G., and Berner, L. (2011). A latitudinal gradient in tree growth response to climate warming in the Siberian taiga. *Glob. Chang. Biol.* 17, 1935–1945. doi: 10.1111/j.1365-2486.2010.02360.x

Lu, X., Liang, E., Camarero, J. J., and Ellison, A. M. (2021). An unusually high shrubline on the Tibetan Plateau. *Ecology* 102:e03310. doi: 10.1002/ecy.3310

Lyu, L., Suvanto, S., Nöjd, P., Henttonen, H. M., Mäkinen, H., and Zhang, Q. (2017). Tree growth and its climate signal along latitudinal and altitudinal gradients: Comparison of tree rings between Finland and the Tibetan Plateau. *Biogeosciences* 14, 3083–3095. doi: 10.5194/bg-14-3083-2017

Matías, L., Linares, J. C., Sánchez-Miranda, Á, and Jump, A. S. (2017). Contrasting growth forecasts across the geographical range of Scots pine due to altitudinal and latitudinal differences in climatic sensitivity. *Glob. Chang. Biol.* 23, 4106–4116. doi: 10.1111/gcb.13627

McDowell, N. G., and Sevanto, S. (2010). The mechanisms of carbon starvation: How, when, or does it even occur at all? *New Phytol.* 186, 264–266.

Morales, A. I. G. C., Mendoza, J. M. O., Gozalbo, M. E., and Martínez, J. J. C. (2012). Arboreal and prostrate conifers coexisting in Mediterranean high mountains differ in their climatic responses. *Dendrochronologia* 30, 279–286. doi: 10.1016/j.dendro.2012.02.004

Myers-Smith, I. H., Forbes, B. C., Wilmking, M., Hallinger, M., Lantz, T., Blok, D., et al. (2011). Shrub expansion in tundra ecosystems: Dynamics, impacts and research priorities. *Environ. Res. Lett.* 6, 21–35. doi: 10.1088/1748-9326/6/4/045509

Myers-Smith, I. H., Hallinger, M., Blok, D., Sass-Klaassen, U., Rayback, S. A., Weijers, S., et al. (2015a). Methods for measuring arctic and alpine shrub growth: A review. *Earth Sci. Rev.* 140, 1–13. doi: 10.1016/j.earscirev.2014.10.004

Myers-Smith, I. H., Elmendorf, S. C., Beck, P. S., Wilmking, M., Hallinger, M., Blok, D., et al. (2015b). Climate sensitivity of shrub growth across the tundra biome. *Nat. Clim. Chang.* 5, 887–892. doi: 10.1038/nclimate2697

Myers-Smith, I. H., Kerby, J. T., Phoenix, G. K., Bjerke, J. W., Epstein, H. E., Assmann, J. J., et al. (2020). Complexity revealed in the greening of the Arctic. *Nat. Clim. Chang.* 10, 106–117. doi: 10.1038/s41558-019-0688-1

Okuda, M., Sumida, A., Ishii, H., Vetrova, V. P., and Hara, T. (2008). Establishment and growth pattern of Pinus pumila under a forest canopy in central Kamchatka. *Ecol. Res.* 23, 831–840. doi: 10.1007/s11284-007-0445-1

Pellizzari, E., Camarero, J. J., Gazol, A., Granda, E., Shetti, R., Wilmking, M., et al. (2017). Diverging shrub and tree growth from the Polar to the Mediterranean biomes across the European continent. *Glob. Chang. Biol.* 23, 3169–3180. doi: 10.1111/gcb.13577

Qian, C., and Zhang, X. (2015). Human influences on changes in the temperature seasonality in mid-to high-latitude land areas. *J. Clim.* 28, 5908–5921. doi: 10.1175/JCLI-D-14-00821.1

R Core Team (2015). *R: A Language and Environment for Statistical Computing*. Vienna: R Foundation for Statistical Computing.

Rosenzweig, C., Karoly, D., Vicarelli, M., Neofotis, P., Wu, Q., Casassa, G., et al. (2008). Attributing physical and biological impacts to anthropogenic climate change. *Nature* 453, 353–357. doi: 10.1038/nature06937

Rossi, S., Anfodillo, T., Èufar, K., Cuny, H., Deslauriers, A., Fonti, P., et al. (2016). Pattern of xylem phenology in conifers of cold ecosystems at the Northern Hemisphere. *Glob. Chang. Biol.* 22, 3804–3813. doi: 10.1111/gcb.13317

Sedlacek, J., Cortés, A. J., Wheeler, J., Bossdorf, O., Hoch, G., Klápště, J., et al. (2016). Evolutionary potential in the Alpine: Trait heritabilities and performance variation of the dwarf willow Salix herbacea from different elevations and microhabitats. *Ecol. Evol.* 6, 3940–3952. doi: 10.1002/ece3.2171

Shao, H., Zhang, Y., Gu, F., Shi, C., Miao, N., and Liu, S. (2021). Impacts of climate extremes on ecosystem metrics in southwest China. *Sci. Total Environ.* 776:145979. doi: 10.1016/j.scitotenv.2021.145979

Shetti, R. (2018). *Potential of Shrubs in the Evolving Field of Arctic and Alpine Dendroecology: Methods in Shrub Dendro-ecology, Understanding the Processes Influencing Shrub Growth in the Arctic and Alpine Ecosystems*. PhD thesis, Greifswald: University of Greifswald.

Vaganov, E. A., Hughes, M. K., Kirdyanov, A. V., and Silkin, P. P. (1999). Influence of snowfall and melt timing on tree growth in subarctic Eurasia. *Nature* 400, 149–151. doi: 10.1038/22087

Weijers, S., Greve, A. I., Bronken, E. P., Broekman, R., Loonen, M. J. J. E., and Rozema, J. (2012). No divergence in Cassiope tetragona: persistence of growth response along a latitudinal temperature gradient and under multi–year experimental warming. *Ann. Bot.* 110, 653–665. doi: 10.1093/aob/mcs123

Wigley, T. M., Briffa, K. R., and Jones, P. D. (1984). On the average value of correlated time series, with applications in dendroclimatology and hydrometeorology. *J. Clim. Appl. Meteorol.* 23, 201–213. doi: 10.1175/1520-0450(1984)023<0201:OTAVOC>2.0.CO;2

Xiao, S. C., Ding, A. J., Tian, Q. Y., Han, C., and Peng, X. M. (2019). Site–and species–specific climatic responses of two co-occurring shrubs in the temperate Alxa Desert Plateau, northwest China. *Sci. Total Environ.* 667, 77–85. doi: 10.1016/j.scitotenv.2019.02.217

Xu, C., Hou, M., Yan, X., and Zhang, X. (2021). Temporal variability of seasonal warming rates in China. *Int. J. Climatol.* 41, e1597–e1607. doi: 10.1002/joc.6793

Yang, J., Cooper, D. J., Li, Z., Song, W., Zhang, Y., Zhao, B., et al. (2020). Differences in tree and shrub growth responses to climate change in a boreal forest in China. *Dendrochronologia* 63:125744. doi: 10.1016/j.dendro.2020.125744

Zhang, X., Bai, X., Hou, M., Chen, Z., and Manzanedo, R. D. (2019). Warmer winter ground temperatures trigger rapid growth of Dahurian larch in the permafrost forests of northeast China. *J. Geophys Res-Biogeo.* 124, 1088–1097. doi: 10.1029/2018JG004882

Zheng, L., Shi, P., Song, M., Zhou, T., Zong, N., and Zhang, X. (2021). Climate sensitivity of high altitude tree growth across the Hindu Kush Himalaya. *For. Ecol. Manage.* 486:118963. doi: 10.1016/j.foreco.2021.118963